

Supplemental Information

An online neural substrate for sense of agency

Valerian Chambon, Dorit Wenke, Stephen M. Fleming,
Wolfgang Prinz, Patrick Haggard

Address correspondence to: Patrick Haggard, Institute of Cognitive Neuroscience, University College London, Alexandra House, 17 Queen Square, London, WC1N 3AR, United Kingdom;
Email: p.haggard@ucl.ac.uk; Phone: +44 (0)20 7679 1153

Inventory of Supplemental Information

1. Supplemental Figures and Tables

Figure S1, related to Figure 1

Figure S2, related to Figure 2

Figure S3, related to Figure 2

Figure S4, related to Figure 2

Figure S5, related to Figure 4

Table S1, related to Figure 2

Table S2, related to Figure 3

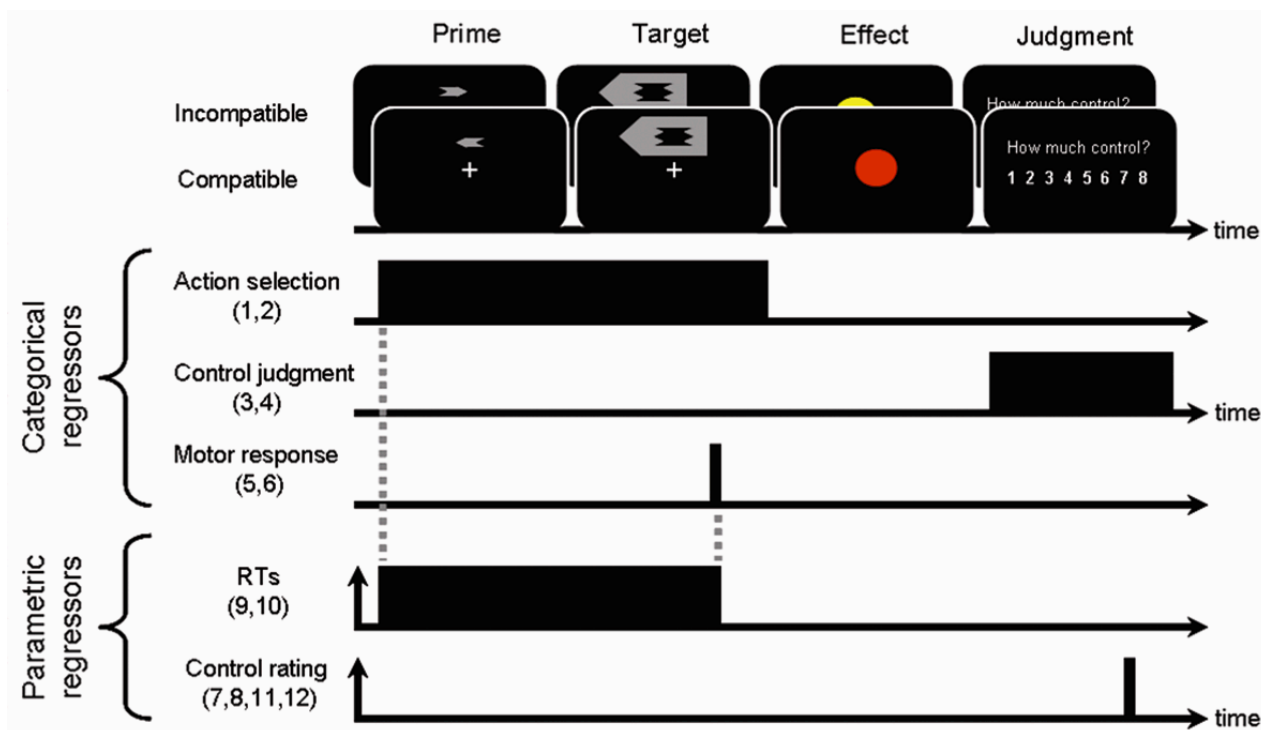
Table S3, related to Figure 4

2. Supplemental Experimental Procedures

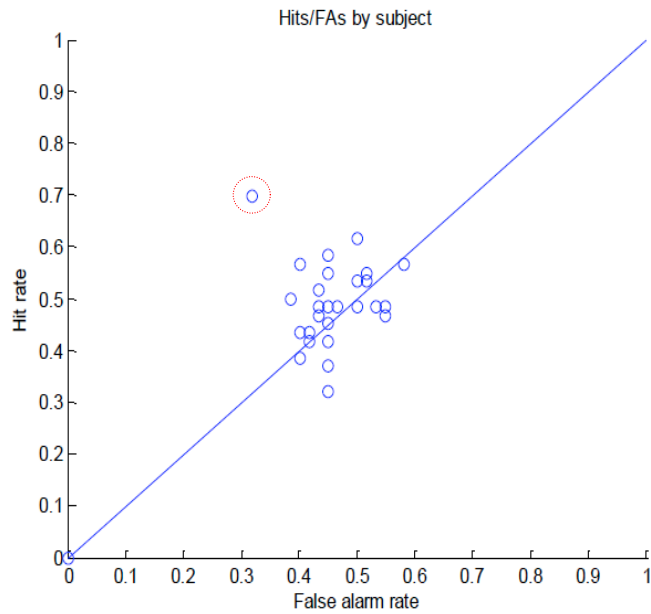
3. Supplemental Results

4. Supplemental References

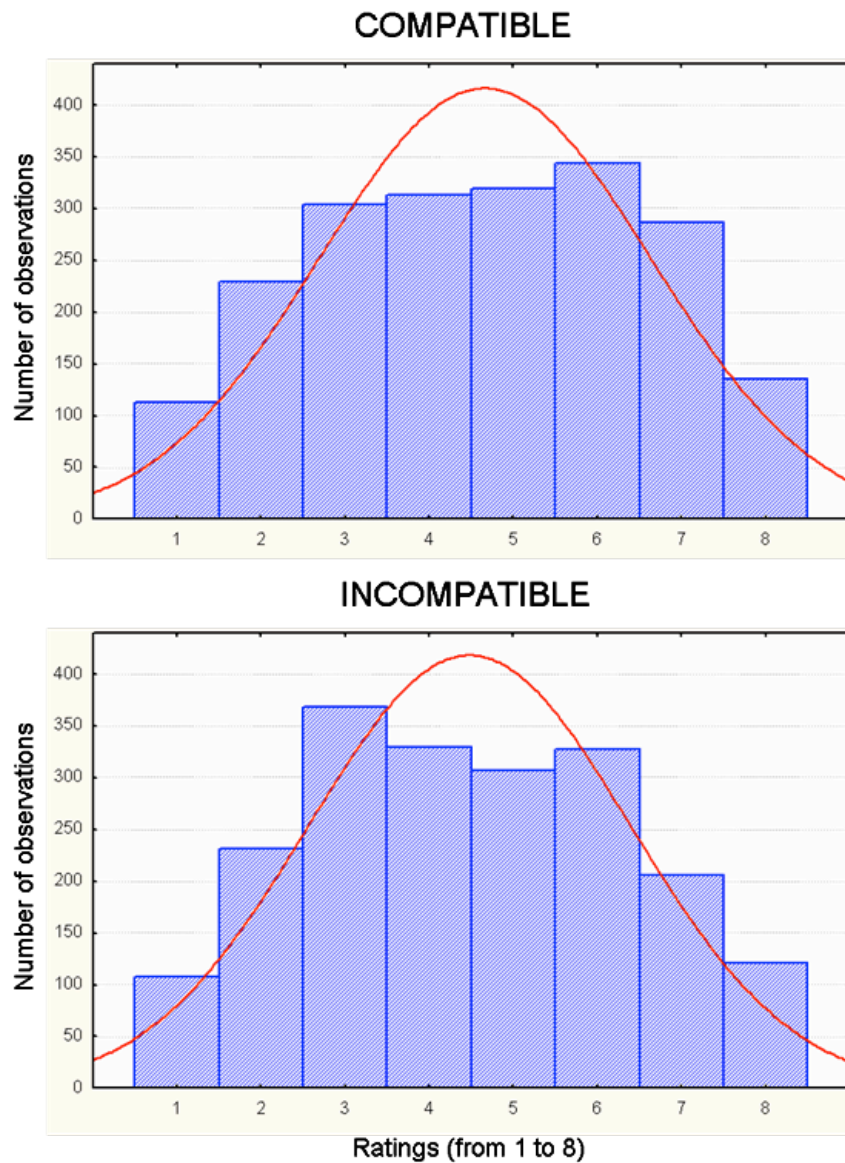
Supplemental Figures and Tables



Supplemental Figure S1. Regressors included in the statistical analysis of fMRI data (related to the experimental design described in Figure 1). The main GLM included six categorical and six parametric regressors (see Supplementary Methods, ‘fMRI data statistical analyses’). The six categorical regressors (1-6) modelled the ‘action selection’ phase, the ‘control judgment’ phase, and the motor response, in both compatible and incompatible trials. Four parametric regressors (7-10) were derived from the ‘action selection’ regressors and hierarchically orthogonalized. These parametric regressors modelled the modulation of BOLD activity at the time of action selection by control ratings (7,8) and RTs (9,10) in compatible and incompatible trials. Two additional parametric regressors were derived from the ‘control judgment’ regressors and modelled the modulation of BOLD activity by control ratings (11,12) in compatible and incompatible trials.



Supplemental Figure S2. Hits/False alarms ratio in the prime visibility test (related to behavioural performances presented in Figure 2). One subject (circled in the plot) was excluded because her d' was sufficiently high (0.98) to suggest conscious perception of the prime (i.e., greater than one standard deviation above the mean). The major diagonal indicates isosensitivity points where hit rate = false alarm rate, and d' is 0.



Supplemental Figure S3. Frequency histograms for control ratings pooled across participants, on compatible and incompatible trials (related to mean control ratings presented in Figure 2). X-axis: the numbers from 1 to 8 refer to the scale used by participants to judge their control over action effects (1 = no control; 8 = complete control). Y-axis: number of observations pooled across participants for each number of the scale. The red curve represents the Gaussian fit for each distribution. Note the shift of the distribution towards lower ratings for incompatible compared to compatible trials.

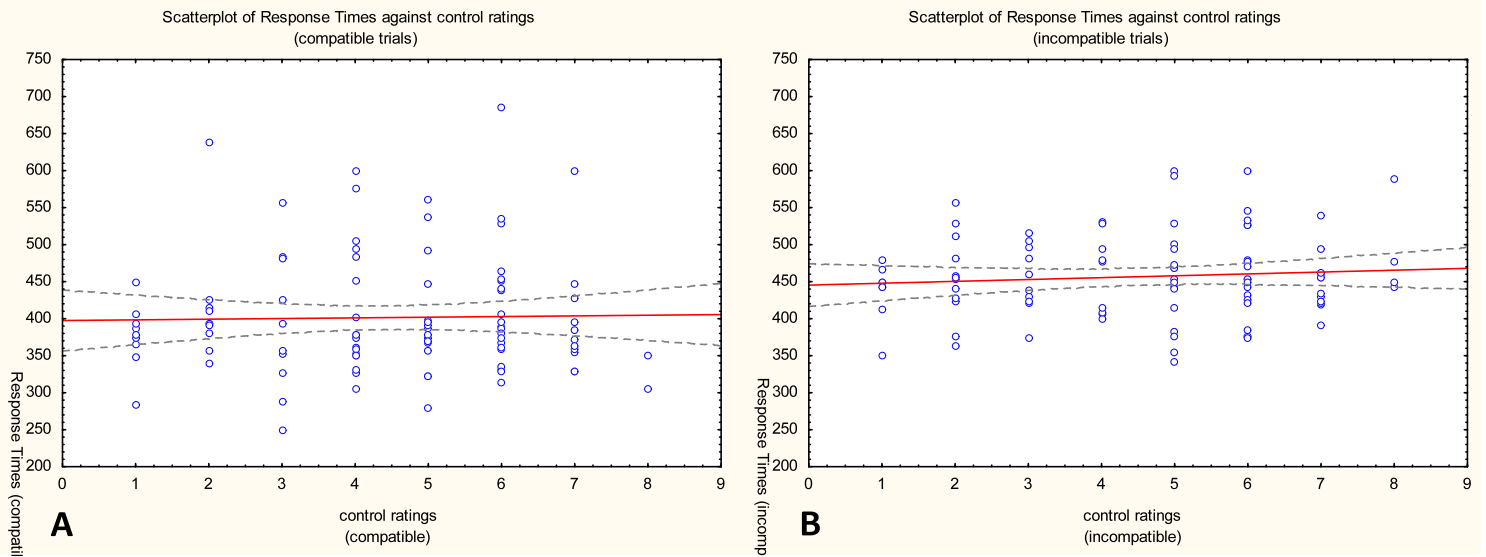
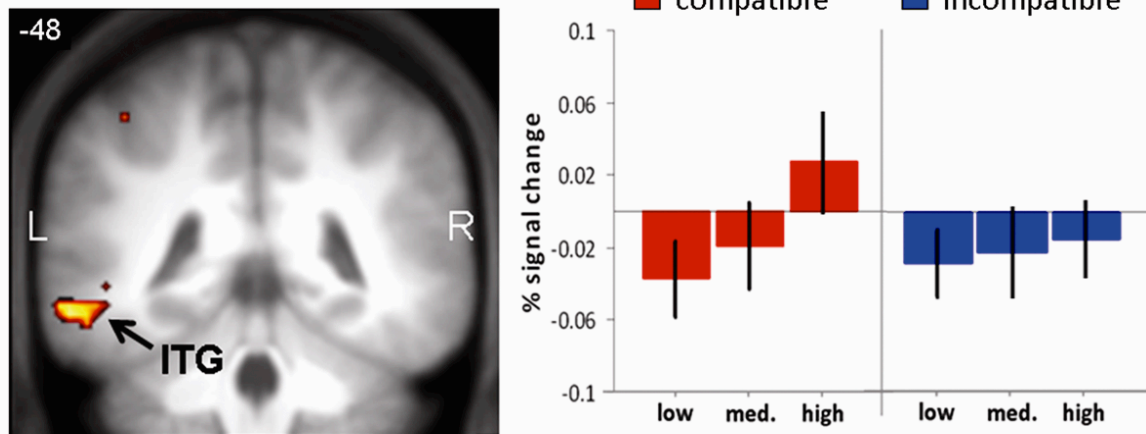


Figure S4. Regression analyses between RTs and control ratings for an illustrative subject (subject 1). The linear regression lines are shown in red. **A.** Compatible trials; **B.** Incompatible trials. The 95% confidence interval (CI) around the regression lines are shown in grey.



Supplemental Figure S5. Left panel: inferior temporal gyrus (ITG) activation ($y = -48$) reflecting the parametric interaction effect between compatibility and control factors at time of action selection (related to Figure 4). Left = Left; R = Right. **Right panel:** percentage of signal change for the three levels of control (low, medium, high) in compatible and incompatible trials. Note that the sign of the interaction (i.e. increased activity in compatible compared to incompatible trials) is opposite to that presented in Figure 4a.

Table S1. Correlation coefficients (R) for the relation between RTs and sense of control ratings for each subject in each priming condition.

	COMPATIBLE	INCOMPATIBLE
SUBJECTS	<i>R value</i>	<i>R value</i>
SUBJ1	0,021	0,09
SUBJ2	0,037	0,101
SUBJ3	0,151	0,133
SUBJ4	0,029	0,192
SUBJ5	0,127	0,06
SUBJ6	0,072	0,073
SUBJ7	0,051	0,056
SUBJ8	0,009	0,018
SUBJ9	0,12	0,136
SUBJ10	0,01	0,054
SUBJ11	0,172	0,116
SUBJ12	0,128	0,045
SUBJ13	0,082	0,025
SUBJ14	0,074	0,08
SUBJ15	0,034	0,011
SUBJ16	0,07	0,021
SUBJ17	0,049	0,161
SUBJ18	0,124	0,051
SUBJ19	0,063	0,024
SUBJ20	0,017	0,032
SUBJ21	0,053	0,019
SUBJ22	0,02	0,032
	<i>all p's > 0.09</i>	<i>all p's > 0.064</i>
AVERAGE	0,068	0,077

Supplemental Table S2. Peak and cluster information for the comparison {compatible > incompatible}, exclusively masked by {compatible*control > incompatible*control}, related to Figure 3. Clusters were defined using a height threshold of $P < 0.001$ and FDR-corrected for multiple comparisons ($P < .05$). Left to right, columns refer to: abbreviation used in the text to refer to significant clusters, coordinate location of the peak in Montreal Neurological Institute space, FDR-corrected p -value at the cluster maximum, T-statistic, volume. L = left; R = right.

Clusters	Coordinates (x, y, z in mm)	FDR-corrected p value	peak T	Volume (mm ³)
R dlPFC	45, 18, 39	0.018	4.62	1485
L dlPFC	-45, 12, 42	0.021	4.32	1584
R OFC	42, 48, -1	0.024	4.09	936
L OFC	-42, 45, 0	0.027	3.85	360
L putamen ^a	-26, -3, 0	0.014	3.77	864

^a Small-volume correction (SVC) was applied by using an anatomical mask for lentiform nucleus as specified in the PickAtlas toolbox (Maldjian et al., 2003).

Supplemental Table S3. Peak and cluster information for the comparison {compatible*control > incompatible*control}, related to Figure 4. From left to right, columns refer to: abbreviation used in the text to refer to significant clusters, coordinate location of the peak in Montreal Neurological Institute space, FDR-corrected p -value at the cluster maximum, T-statistic, volume. L = left; R = right.

Clusters	Coordinates (x, y, z in mm)	FDR-corrected p value	peak T	Volume (mm ³)
L AG	-36, -69, 45	0.014	4.47	1728
L ITG	-57, -48, -12	0.017	4.41	1296
Cerebellar vermis	0, -48, -12	0.26	3.68	504

Supplemental Experimental Procedures

Action-effect experiment: apparatus and materials

The visual display was presented on a screen (display mode= 800 × 600 × 32, 60 Hz) positioned at the front of the magnet bore. Subjects lay supine in the scanner and viewed the display on a mirror positioned above them. The experiment was programmed and stimulations were delivered using the software Presentation (Neurobehavioral Systems, Albany, California, <http://www.neurobs.com>). Primes consisted of grey left or right pointing arrows that were followed and superimposed by metacontrast masks of the same luminance. The metacontrast masks also consisted of arrows that pointed to the left or the right (see **Figure 1**). Participants responded to the masks with keypress actions. Prime and mask stimuli could appear randomly above or below fixation to enhance the masking effect (Vorberg et al., 2003). Effects were circular colour patches of red, green, blue, or yellow. All stimuli appeared on a grey background. Participants made left or right keypress actions on each trial using the index fingers of their left and right hands, and made control ratings using all fingers of each hand, with the exception of thumbs. To respond to targets as to make their control judgments, participants used two 4-buttons response-boxes placed in their left and right hands.

Examples of each (left and right) mask stimulus were presented during experimental instruction so that participants would become acquainted with the target stimuli. No reference was made to the existence or appearance of the primes.

Prime-visibility test

Following the action–effect experiment, each participant additionally performed a direct assessment of prime visibility inside the scanner. Defining criteria for non-conscious perception is fraught with debate (Erdelyi, 2004). Criteria can be either subjective (based on self-report) or objective (based on cued-choice performance). As our aim in this investigation was to ensure the unconscious nature of our prime stimuli, we selected the more conservative, objective criterion of awareness. Furthermore, to ensure that the prime visibility test was a valid measure of prime perception during the action–effect experiment, we matched the task designs in as many ways as possible (Schmidt & Vorberg, 2006). Participants were explicitly informed of the presence of the prime, and asked to identify its direction on each trial (left or right) using a left or right keypress. Other elements of the trial sequence remained identical to the action-effect experiment (see **Figure 1**), except that the effect itself was not presented. However, these stimuli were irrelevant to the prime detection task. To ensure that conscious judgement of the prime direction was not contaminated by the unconscious activation of the compatible response, participants were only permitted to report 600 ms after the mask had appeared (Vorberg et al., 2003). The start of the reporting interval was signalled by a 1000 Hz tone played for 150 ms. The prime visibility test consisted of two blocks of 60 trials each. Responses to the primes were categorised using the framework of signal detection theory (Green & Swets, 1966) allowing us to compute a measure of prime discriminability (d') for each subject (see **Figure S2**).

fMRI data statistical analyses

Twelve task regressors were entered in our general linear model (GLM), including 6 categorical and 6 parametric regressors (see **Figure S1**). Categorical regressors modelled BOLD activity related to: action selection in compatible (1) and incompatible (2) trials; control judgment in compatible (3) and incompatible (4) trials; motor response in compatible (5) and incompatible (6) trials. Four parametric regressors were added to the “action selection” regressors to account for modulation of BOLD signal by control in compatible (7) and incompatible (8) trials, and by participants’ RTs in compatible (9) and incompatible (10) trials as well. Finally, two parametric regressors were added to the “control judgment” regressors to account for modulation of BOLD signal by control in compatible (11) and incompatible (12) trials.

For illustrative purpose, we used the `rfx_plot` toolbox (Gläscher, 2009) to split parametric regressors accounting for the modulation of BOLD activity by control at time of action selection into 6 new onsets regressors, each containing all events for a particular tertile of control in each compatibility condition ($2\{\text{compatible, incompatible}\} \times 3\{\text{low, medium, high}\} = 6$). Beta weights were re-estimated for each of these 6 onset regressors and averaged across all subjects to get corresponding % of signal change (see **Figure 4a**, right panel).

Functional connectivity analyses procedure

We tested whether brain regions demonstrating a main effect of *compatibility* (i.e., dlPFC, OFC, and left putamen) showed context-dependent changes (i.e., changes depending on compatibility of incompatibility of action selection) in coupling with the region showing a parametric effect of *control* (i.e., left Angular Gyrus) by conducting separate psycho-physiological interactions (PPI) (Friston et al., 1997).

The individual time series for left AG were obtained by extracting the first principal component from all raw voxel time series in a sphere (4-mm radius) centred on the coordinates of the AG group-level activations. Using standard analysis techniques, these “physiological” time series were corrected for variance associated with parameters of no interest, deconvolved with the haemodynamic responses function (Gitelman et al., 2003), multiplied by a parameter encoding the relevant “psychological” contrast (e.g., 1 for parametric effect of control in compatible trials, -1 for parametric effect of control in incompatible trials, 0 elsewhere), and reconvolved to form a “psychophysiological interaction” (PPI) regressor. The PPI regressor was mean-corrected and orthogonalized with regard to the main effect of task (psychological regressor) and the corresponding time series (physiological regressor).

As mentioned above, potential brain sites for contextual AG influences were regions showing a main effect of compatibility at time of action selection (i.e., dlPFC and OFC, bilaterally, and left putamen). Within a functional mask (uncorrected voxelwise threshold $P < .05$) defined by these activations (WFU PickAtlas software; Maldjian et al., 2003), we determined which sites received contextual AG influences that were stronger in compatible than in incompatible trials (and conversely). This was done by testing for positive or negative slopes of the PPI regressor, i.e., by applying a t -contrast that was 1 (positive slope) or -1 (negative slope) for the PPI regressor, and 0 elsewhere. Subject-specific contrast images were then entered into random effects group analyses.

Supplemental Results

Interaction between compatibility and sense of control at the time of action selection

At time of action selection, the left inferior temporal gyrus (ITG) showed a significant compatibility \times control interaction effect, with activity increasing with greater control in *compatible* trials (MNI coordinates of maximal random-effect T scores, $x, y, z = -57, -48, -12, T = 4.41$) (see **Figure S4** and **Table S2**).

Interaction between compatibility and sense of control at the time of control judgment

At time of control judgment, a compatibility \times control interaction effect was found in voxels within the supplementary motor area (SMA) ($x, y, z = 6, -12, 60, T = 4.14$), with activity decreasing with greater control in *incompatible* trials. This activation, however, did not survive FDR correction for multiple comparisons ($P < 0.05$).

Supplemental References

Erdelyi, M. (2004). Subliminal perception and its cognates: Theory, indeterminacy, and time.

Consciousness and Cognition, 13, 73–91.

Friston, K.J., Buechel, C., Fink, G.R., Morris, J., Rolls, E., Dolan, R.J. (1997).

Psychophysiological and modulatory interactions in neuroimaging. *Neuroimage* 6, 218-229.

Gitelman, D.R., Penny, W.D., Ashburner, J., Friston, K.J. (2003). Modeling regional and psychophysiologic interactions in fMRI: the importance of hemodynamic deconvolution.

Neuroimage 19, 200-207.

Gläscher, J. (2009). Visualization of Group Inference Data in Functional Neuroimaging,

Neuroinformatics 7: 73-82.

Green, D. M., and Swets, J. A. (1966). Signal detection theory and psychophysics. New York:

Wiley.

Maldjian, J.A., Laurienti, P.J., Kraft, R.A., Burdette, J.H. (2003). An automated method for neuroanatomic and cytoarchitectonic atlas-based interrogation of fMRI data sets.

Neuroimage 19, 1233-1239

Schmidt, T., and Vorberg, D. (2006). Criteria for unconscious cognition: Three types of dissociations. *Perception and Psychophysics*, 68, 489–504.

